Multi-modes locomotion on natural terrain

Faiz Ben Amar, Christophe Grand, Guillaume Besseron, Frédéric Plumet

Multi-modes locomotion on natural terrain

F. Ben Amar, Ch. Grand, G. Besseron, F. Plumet
Laboratoire de Robotique de Paris (LRP)
Université Pierre et Marie Curie, Paris 6 - CNRS FRE 2507
18 route du Panorama - BP61 - 92265 Fontenay-aux-Roses, France
{*amar,grand,besseron,plumet*}*@robot.jussieu.fr*

Abstract

This study deals with performance evaluation of locomotion modes of a redundant off-road robot in order to adapt the locomotion parameters to ground conditions. Evaluation criterion which are stability, gradeability and energy consumption of each locomotion mode are studied for different mechanical terrain parameters. The proposed evaluation framework is based on quasi-static motion equations and includes basic concepts of Terramechanics.

Keywords
multi-modal locomotion, wheel-legged robot, gradeability, stability, controllability, power consumption.

1 Introduction

One of the key factor for success of future autonomous planetary exploration missions could be the use of rovers with high locomotion performance. During the last decades, many researches were dedicated to the design of what so-called "high mobility systems". This concept is referred to both speed capacity and clearance ability. The classical trends for high mobility rovers consists in integrating internal mobility into conventional wheeled systems in order to overcome their main handicap i.e. the insufficiency of clearance capacity. These mobilities could be : (1) passive (unactuated joint or with spring-damper device) as for the Rocky rovers [12], Shrimp [11], Nomad [10] and Nexus [13]; or (2) active (actuated joint) as for SRR [8], Azimut [9], HyLoS [4] and WorkPartner [7]. Those three last robots are able to perform different locomotion modes, based on a mix between rolling and crawling gait, which offer the possibility to adapt the mode to the local terrain difficulty. This adaptation requires obviously an identification of both geometrical and physical terrain properties.

This paper deals with the performance evaluation of locomotion modes of the wheel-legged Hylos robot as function of some significant terrain parameters. The chosen evaluation criterion depict the configuration safety, the clearance capacity and the energy consumption. First, we will describe the mechatronic architecture of the Hylos robot and the associated locomotion modes. Next, we will develop basic models used in the evaluation process of the different locomotion modes. Finally, some preliminary results of evaluation criteria will be presented for each locomotion modes as function of different terrain properties.

2 Hylos description and associated locomotion modes

Hylos (fig.1) is a wheel-legged robot with 16 degrees of freedom. It is approximately 70 cm long and weights 12 kg. It has four legs each combining a 2 degree-of-freedom suspension mechanism with a steering and driven wheel. Each leg is composed of two 20 cm length link driven by two electrical linear actuators and the wheel radius is 6 cm. This mechanism can be seen as a large displacement active suspension. Hylos is equipped with two inclinometers to get the platform pitch and roll angles and 3 axes forces sensor on each leg for contact force measurement. Four control-boards based on a 80c592 micro-controller are dedicated to the low-level control of each leg (four DOF controlled by each one). A PC-104 board is used for high-level posture control (and also the other locomotion modes: rolling motion, peristalsis motion, ...). Communications between the PC and micro-controllers are achieved through a CAN bus.

A new similar platform, Hylos 2, is currently developed and will be equipped with stereo vision system. This enables ground surface mapping and soil material characterization by image texture analysis. These models are used in a supervisor which have to select the locomotion mode the most appropriate with respect to the ground conditions. Figure (1.b) depicts the general control scheme of the robot. The internal loop is dedicated for low level control of each locomotion mode and the external one for mode selection.

We consider in this paper 3 locomotion modes for the Hylos rover, of which definitions are given in the following items.

- (M1) is the pure rolling mode, with the legs mo-

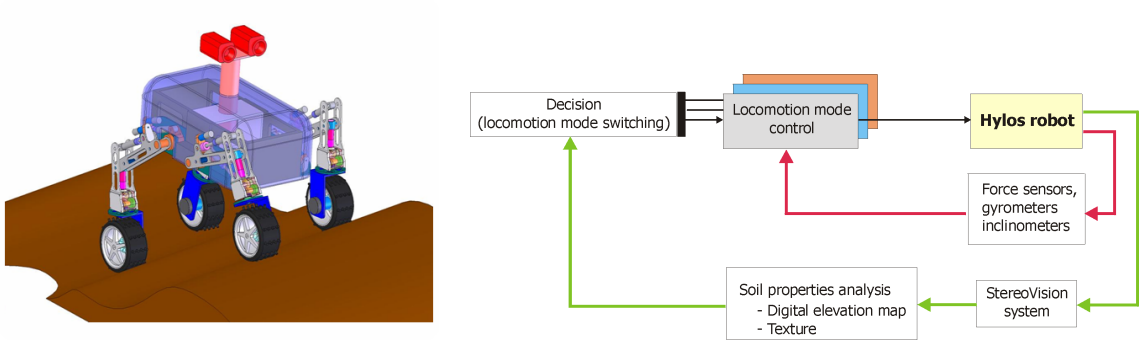

(a) (b)

Figure 1: (a) View of Hylos 2 - (b) Global control scheme of Hylos robot

bilities locked in their nominal configuration. This mode is convenient for flat and smooth hard ground.

- (M2) is the rolling with reconfiguration mode. In this case, the internal active mobilities are used to optimize the posture in order to enhance the locomotion performance. The used criteria are the tipover stability margin and the wheel-ground contact force balance. A suboptimal posture of the robot that optimize the normal component of contact force is defined [5]. The normal forces balance is optimized by assuming the distribution of vertical component of contact forces. Because of the particular design of Hylos, this corresponds to maintain the roll angle to zero, and to configure each leg in such way that projected distances between contact points and the platform center of gravity are equal. The other posture parameters that are the ground clearance, the pitch angle and the nominal wheelbase are specified by a high level controller with respect to the platform task (vision, manipulation). This locomotion mode is adapted to irregular ground without discontinuities like sloping ground or rough terrain. Figure (2.a) depicts Hylos evolving on an asymmetric irregular ground with maintaining constant its configuration (roll and pitch angles and platform height). Figure (2.b) represents the roll and picth angles as function of time in this mode (M2) whereas curves of (fig.2.c) are of those angles in pur rolling mode (M1) for the same ground profile and which gives critical instable configurations of the rover.

- (M3) is the crawling mode which is mainly based on legs mobilities to produce traction force. Different gaits could be defined from biological quadruped or from worms (peristaltic symmetric mode). In this study, we choose one cyclic gait in which each pair of wheels in the frontal plane moves only when the other one is firmly braced to the ground (see Fig.3). Because of minimizing rolling resistance due to ground compaction, this mode is well adapted for locomotion on non-cohesive soft soils as sand or any other granular material [1].

3 Kineto-static motion model with basic terramechanics concepts

We present in this section the models used for a qualitative evaluation of the considered locomotion modes as function of the terrain parameters. We assume a quasi-static motion of the system with permanent ground contact. Slippage are considered through terramechanics equations.

First, the general formulation of kineto-static motion of the system is expressed by, first the velocity equation

$$\mathbf{L}\mathbf{v}_p = \mathbf{J}\dot{\mathbf{q}} + \mathbf{v}_s \tag{1}$$

and the equilibrium equations

$$\mathbf{L}^t\mathbf{f} = \mathbf{g} \tag{2}$$

$$\mathbf{J}^t\mathbf{f} = \boldsymbol{\tau} + \mathbf{h} \tag{3}$$

In these equations:

- $\mathbf{L}$ is a 12x6 locomotion matrix,
- $\mathbf{J}$ is 12x16 jacobian matrix,
- $\mathbf{v}_p$ is vector of the twist components of the platform;
- $\dot{\mathbf{q}}$ is vector of joint rates,
- $\mathbf{v}_s = [\mathbf{v}_{si}]$ is vector of slippage velocities along each contact frame $\mathcal{R}_i = (C_i, \mathbf{t}_i, \mathbf{l}_i, \mathbf{n}_i)$, where $\mathbf{n}_i$ is the normal vector to ground at the contact point C_i, $\mathbf{t}_i$ is the longitudinal vector, $\mathbf{l}_i$ is the lateral vector,
- $\mathbf{f} = [\mathbf{f}_i]$ is vector of contact components,
- $\mathbf{g}$ is vector of generalized force due to gravity associated to platform displacement ,

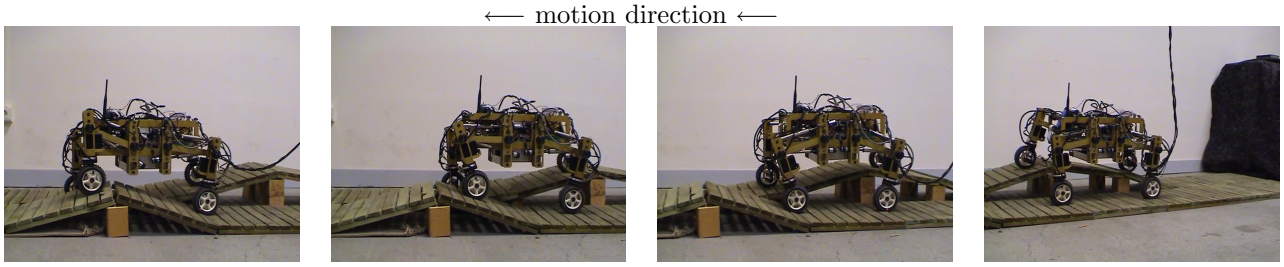

(a) Hylos 1 evolving on an irregular ground profile with a constant nominal configuration (Mode 2).

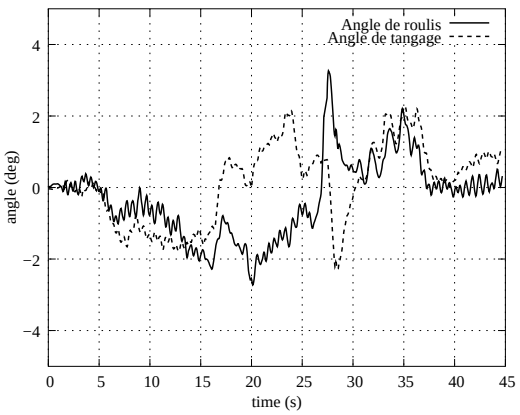

(b)

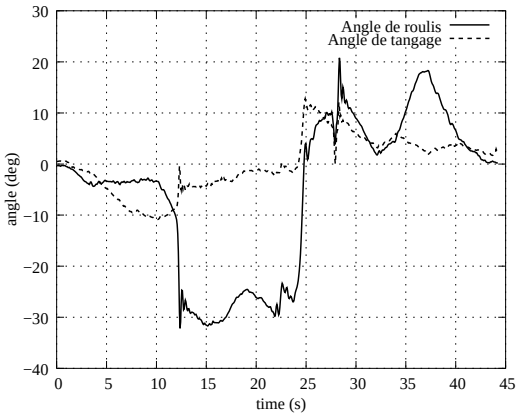

(c)

Figure 2: (b) Roll and pitch angles in mode 2, (c).Roll and pitch angles in mode 1.

- $\mathbf{h}$ is vector of generalized force associated joint parameters;
- $\boldsymbol{\tau}$ is vector of joint torques.

The contact force under each wheel expressed in the local frame is defined by $\mathbf{f}_i = [T_i - R_i, L_i, W_i]^t$, where

- T_i is thrust force,
- R_i is the rolling resistance,
- L_i is the lateral force,
- W_i is the normal load.

We use classical Bekker's equations for rigid wheel to express the rolling resistance[3]:

$$R_i = b\left[(k_c/b + k_\phi)\frac{z_i^{n+1}}{n+1}\right] \tag{4}$$

with

$$z_i = \left[\frac{3W_i}{b(3-n)(k_c/b+k_\phi)\sqrt{D}}\right]^{\left(\frac{2}{2n+1}\right)} \tag{5}$$

In these equations,

- z_i is wheel sinkage,
- b is the wheel width,
- k_c, k_ϕ, n are Bekker's terrain parameters in relation with terrain response to a vertical load.

We use the slip-drift theory introduced in [6] to express the thrust and lateral components

$$\begin{cases} T_i = V_i \cos\beta_i \\ L_i = V_i \sin\beta_i \end{cases} \tag{6}$$

with

$$\begin{cases} V_i = (A_i c + W_i \tan\phi)\Big(1 - \dfrac{K}{u_i l}\big(1 - \exp(\dfrac{-u_i l}{K})\big)\Big) \\ \beta_i = \arctan\big(\dfrac{1-s_i}{s_i}\tan\alpha_i\big) \\ u_i = \sqrt{(1-s_i)^2\tan^2\alpha_i + s_i^2} \end{cases} \tag{7}$$

In these equations :

- s_i is the slippage ratio,
- α_i is the drift angle,
- c the soil cohesion,
- ϕ the internal friction angle,
- K the shear modulus,

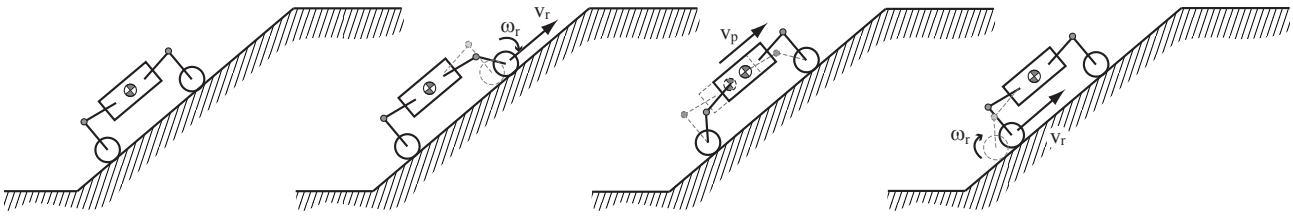

Figure 3: Sequences of crawling with a 2D symmetric gait (Mode 3).

- V_i is the total tangential force;
- β_i is the tangential force angle,
- u_i is the rate of change of displacement in the contact area,
- $A_i = bl_i$ is the contact area with l_i the contact length.

The static equation of the vehicle, considered as a rigid system, is undetermined. This indeterminacy is due to the fact that the system has a non-minimal number of contact with the environment. Moreover, these contacts are frictional. Another source of indeterminacy comes from the use of redundant actuation. The equilibrium equations of the system (first part of equation 3) have a general solution equal to:

$$\mathbf{f} = (\mathbf{L}^t)^+\mathbf{g} + (\mathbf{I} - \mathbf{L}^t\mathbf{L})\boldsymbol{\lambda} \tag{8}$$

where $(\mathbf{L}^t)^+$ is the generalized inverse matrix and $\boldsymbol{\lambda}$ is an arbitrary vector. Thus, to solve the indeterminacy, we use an optimization procedure based on the simplex method to find a solution that minimizes the tangential force ratios T_i/W_i and L_i/W_i. This solution leads to maximize the traction efficiency and to minimize the drift angle.

4 Preliminary results on performance evaluation

This section try to quantify some performance criterion which express the locomotion mobility of the Hylos robot as function of some terrain parameters. We remind that the goal is to adapt the locomotion modes to terrain conditions. The selection of the appropriate mode could be based on some rules which considers many performance criterion as function of the mission constraints. We will assume in this study that both geometrical and mechanical properties of ground are known. The results, presented in this section, are proper to Hylos robot. The method considers specific geometry and actuation constraints of our robot and can not be automatically generalized to the same locomotion modes of another system. Nevertheless, the presented results have some general physical meanings in a qualitative point of view.

We will consider first the stability criteria through a margin stability analysis. Next, we will study the gradeability (i.e. the maximum slope that a vehicle can climb without compromising the vehicle's stability or it's ability to move forward). Finally, we will look at the power consumption criteria.

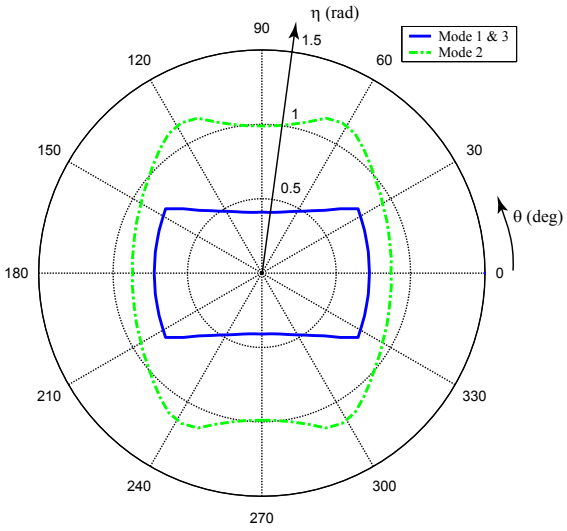

Figure 4: Stability evaluation of locomotion modes on slopping ground with different yaw angles.

4.1 Evaluation of stability

We use here the stability margin as defined in [2] on a slopping ground with different configuration angles. Figure (4) represents the stability margin limit (equal to 0.1 rad.) on a polar graph where the radius η depicts the slope angle and the polar angle θ is the robot yaw angle with respect to the slope direction. As seen on this figure, mode 3 has the same limit as mode 1 since a crawling sequence comes through the nominal configuration. Obviously, mode 2 offers high stability perfor-

Terrain type	n	K_c (kN/m^{n+1})	k_ϕ (kN/m^{n+2})	c (kPa)	ϕ (deg)	K (mm)
(1) Dry sand	1.10	0.99	1528	1.04	28.0	11.4
(2) LETE sand	0.79	102.00	5301	1.30	31.1	11.3

Table 1: Parameters of terrain types (1) and (2).

mance with reference to other modes, and particularly when the robot has a side angle with the maximum slope. The non-smooth behavior of curves in mode 1 and 3 comes from the switch of the tipover axis from rearwards to sidewards; however for curve of mode 2, it is mainly due to the limits of the leg workspace.

4.2 Evaluation of gradeability

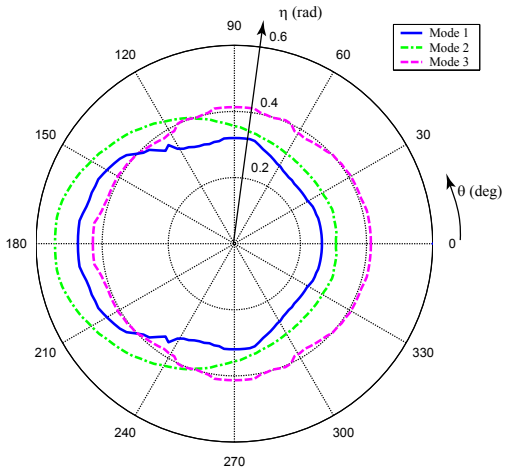

Terrain type 1

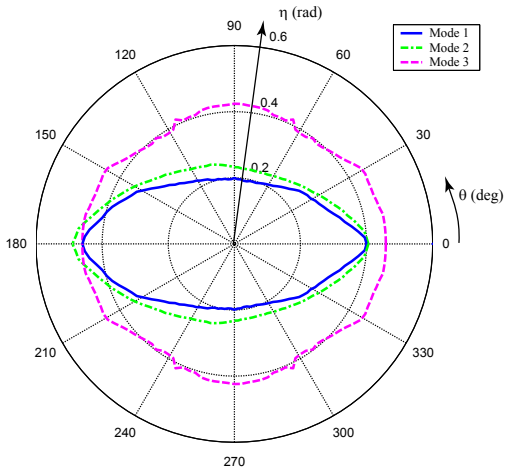

Terrain type 2

Figure 5: Gradeability evaluation of locomotion modes.

Gradeability is usually defined as the maximum slope η that the vehicle can climb. We extend this concept to any yaw angle θ on slopes. We define it as the limits domain of the parameters η, θ where both slippage ratio s_i and drift angle α_i remains acceptable. Here the ground mechanical properties are of first importance. Figure (5) represents on a polar graph, as for stability curves given in the previous section, the gradeability limits for terrain type 1 and type 2 of which parameters are given in table (1). In this case, limits of 0.5 for s_i and 15° for α_i are considered. We observe that crawling mode has good performance for climbing slopes. The main advantage of this mode is that it minimizes rolling traction and so reduces rolling resistance due to ground compaction. This mode does not depend on yaw angle, oppositely to other modes. In modes 1 and 2, the lateral force produced in side configuration affects completely the gradeability performance of the system, especially on terrain with high stiffness (high value of K_c and K_ϕ). This is true only for rigid wheel, as considered by here by Bekker's equation, for which the contact area on hard ground is relatively small. Furthermore, the curves are not symmetric with respect to vertical axis ($\theta = \pm 90°$), as the rolling resistance contributes to improve the gradeability when the vehicle is going down the slope.

4.3 Evaluation of energy Consumption

In this section, the energy consumption of the vehicle climbing on a frontal slope ($\theta = 0°$) is analyzed for each mode and for the two terrains listed in Table 1. The curves in figure (6) represent the energy per traveled distance as function of slope angle η. We can notice that the mode 1 is the most efficient for small slope angle, whereas the crawling mode becomes more efficient after a certain critical angle η_c. As for gradeability, this can be explained by considering that the rolling resistance reduces the traction capabilities in modes 1 and 2. The energy consumption increases greatly after a certain limit that corresponds to the boundary of gradeability domain, as the slippage tends toward its maximal value 1 ($s_i \to 1$). The critical angle η_c for the terrain type 2 is greater than for terrain type 1. In fact, the terrain type 2 is harder (the equivalent vertical stiffness $K_\phi + K_c/b$ is greater) and consequently the wheel sinkage and the rolling resistance are less important.

5 Conclusion

A framework for evaluation of locomotion modes is presented in this paper and is applied to the redundant

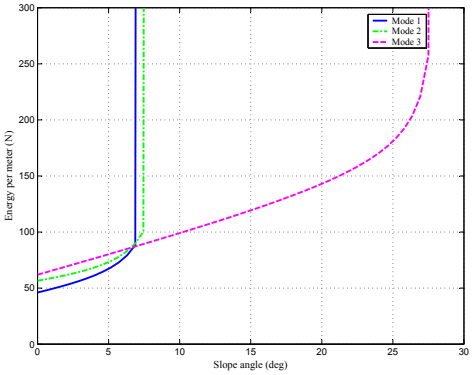

Terrain type 1

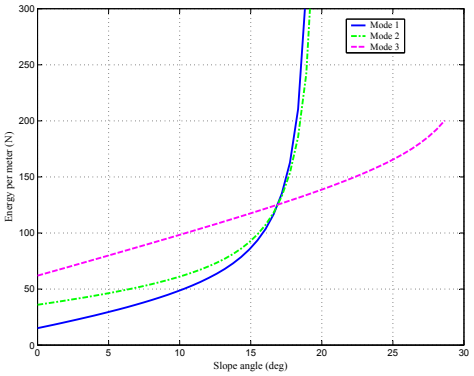

Terrain type 2

Figure 6: Energy consumption of locomotion modes as function of slope angle.

wheel-legged robot Hylos. Some preliminary results are presented for comparison of performances criterion (stability, gradeability and energy consumption) of each mode as function of terrain parameters. This work is carried out in order to provide on-line self adaptation of the locomotion parameters to ground conditions. For unknown environment applications, soil type will be determined qualitatively from textural analysis of images captured by the robot. Embedded proprioceptive sensors (force, acceleration, GPS,...) will be used for an estimation of terrain parameters. Future works will consider other terrain conditions such as amplitudes and frequencies of terrain profile. This should be based on dynamic analysis of the stability margin. This study will be continued in order to establish general rules for optimal multi-modal locomotion on uneven terrain.

References

[1] G. Andrade, F. BenAmar, Ph. Bidaud, and R. Chatila. Modeling wheel-sand interaction for optimization of a rolling-peristaltic motion of a marsokhod robot. In *Int. Conference on Intelligent Robots and Systems*, pages 576–581, 1998.

[2] D. Apostolopoulos. *Analytical Configuration of Wheeled Robotic Locomotion.* Phd thesis, Carnegie Mellon University, 2001.

[3] M.G. Bekker. *Introduction to terrain-vehicle systems.* The University of Michigan Press, 1969.

[4] C. Grand, F. BenAmar, F. Plumet, and P. Bidaud. Decoupled control of posture and trajectory of the hybrid wheel-legged robot hylos. In *IEEE Int. Conference on Robotics and Automation*, pages 5111–5116, 2004.

[5] C. Grand, F. BenAmar, F. Plumet, and P. Bidaud. Stability and traction optimisation of a reconfigurable wheel-legged robot. In *to be published in the International Journal of Robotics Research*, Oct. 2004.

[6] A. Grecenko. Some applications of the slip and drift theory of the wheel. In *Proc. of the 5th Int. Conf. of Society of Terrain Vehicle Systems*, Detroit, USA, 1975.

[7] A. Halme, I. Leppänen, S. Salmi, and S. Ylönen. Hybrid locomotion of a wheel-legged machine. In *3rd Int. Conference on Climbing and Walking Robots (CLAWAR'00)*, 2000.

[8] K. Iagnemma, A. Rzepniewski, S. Dubowsky, and P. Schenker. Control of robotic vehicles with actively articulated suspensions in rough terrain. *Autonomous Robots*, 14(1):5–16, 2003.

[9] F. Michaud and al. Azimut: a leg-track-wheel robot. In *IEEE Int. Conference on Intelligent Robots and Systems*, pages 2553–2558, 2003.

[10] E. Rollins, J. Luntz, A. Foessel, B. Shamah, and W. Whittaker. Nomad: a demonstration of the transforming chassis. In *IEEE Int. Conference on Robotics and Automation*, pages 611–617, 1998.

[11] R. Siegwart, P. Lamon, T. Estier, M. Lauria, and R. Piguet. Innovative design for wheeled locomotion in rough terrain. *Robotics and Autonomous Systems*, 40:151–162, 2002.

[12] R. Volpe. Rocky 7: A next generation mars rover prototype. *Journal of Advanced Robotics*, 11(4):341–358, 1997.

[13] K. Yoshida and H. Hamano. Motion dynamics of a rover with slip-based traction model. In *IEEE Int. Conference on Robotics and Automation*, pages 3155–3160, 2002.